Available online at www.sciencedirect.com
ScienceDirect
Chinese Journal of Aeronautics 23(2010) 501-510
Chinese Journal of Aeronautics
www.elsevier.com/locate/cja

Grindability and Surface Integrity of Cast Nickel-based Superalloy in Creep Feed Grinding with Brazed CBN Abrasive Wheels

Ding Wenfeng*, Xu Jiuhua, Chen Zhenzhen, Su Honghua, Fu Yucan

College of Mechanical and Electrical Engineering, Nanjing University of Aeronautics and Astronautics, Nanjing 210016, China

Received 4 December 2009; accepted 14 January 2010

Abstract

The technique of creep feed grinding is most suitable for geometrical shaping, and therefore has been expected to improve effectively material removal rate and surface quality of components with complex profile. This article studies experimentally the effects of process parameters (i.e. wheel speed, workpiece speed and depth of cut) on the grindability and surface integrity of cast nickel-based superalloys, i.e. K424, during creep feed grinding with brazed cubic boron nitride (CBN) abrasive wheels. Some important factors, such as grinding force and temperature, specific grinding energy, size stability, surface topography, microhardness and microstructure alteration of the sub-surface, residual stresses, are investigated in detail. The results show that during creep feed grinding with brazed CBN wheels, low grinding temperature at about 100 °C is obtained though the specific grinding energy of nickel-based superalloys is high up to 200-300 J/mm^3. A combination of wheel speed 22.5 m/s, workpiece speed 0.1 m/min, depth of cut 0.2 mm accomplishes the straight grooves with the expected dimensional accuracy. Moreover, the compressive residual stresses are formed in the burn-free and crack-free ground surface.

Keywords: grinding; superalloys; brazed abrasive wheels; cubic boron nitride; surface integrity

1. Introduction

Cast nickel-based superalloys are a diverse group of materials, commonly used for elevated temperature application, in which high strength, excellent corrosion resistance and good fatigue resistance are required[1]. Their major application is in the gas and steam turbines components and aircraft engine component construction. However, the high strengths at elevated temperatures, high work hardening, and low thermal diffusivity are generally associated with the poor grindability of nickel-based superalloys. It always leads to high temperatures at the grinding zone and possible thermal damage to the workpiece during grinding with abrasive wheels[2-3].

Previous research has discovered that the technique of creep feed grinding is a promising machining process because it combines the advantage of high shape accuracy, which is the character of conventional grinding, and the merit of high material removal rate, which is the quality of tool cutting[4]. Large depth of cut, long arc of cut and very slow workpiece speed are the predominant features of the creep feed grinding process. In theory, it could offer high productivity and surface finish for components with complex profiles. At present, creep feed grinding technique has been applied to machining nickel-based superalloys, titanium alloys, SiC and Si_3N_4 ceramics, cemented tungsten carbide materials using electroplated cubic boron nitride (CBN) abrasive wheels, resin-bonded diamond wheels and vitrified bonded SiC abrasive tools[4-7]. Whereas, the thermal damage of the machined materials and the drastic wear of the abrasive wheels have constituted the major problems in the creep feed grinding process. In particular, premature grain pullout behavior from the tool substrate under the heavy loads has been one of the important wear patterns[8-9].

On the other hand, monolayer brazed-type CBN grinding wheels have outperformed the widely used electroplated and vitrified counterparts[10-12]. The reason is that, a precision brazing process builds a chemical bridge between CBN grains and tool substrate with the help of an active braze alloy, i.e. Ag-Cu-Ti alloy. The brazed abrasive tools have the strong potential to realize high efficiency grinding of difficult-to-cut ma-

*Corresponding author. Tel.: +86-25-84892901.
E-mail address: dingwf2000@vip.163.com
Foundation items: National Basic Research Program of China (2009CB724403); Program for Changjiang Scholars and Innovative Research Team in University (IRT0837); Program for New Century Excellent Talents in University from Ministry of Education of China (NCET-07-0435)

doi: 10.1016/S1000-9361(09)60247-8

terials owing to the high bonding strength of abrasive grains and the sufficient storage space for chips. In recent years, great achievements have been made for the development of brazed CBN wheels. The CBN abrasive wheels were manufactured using Ag-Cu-Ti alloy as the bond material at 920 °C for 5 min. The interfacial microstructure of CBN grains/bond material and bond material/tool substrate was investigated. The chemical resultants of CBN grain and filler alloy containing Ti were identified as TiB_2, TiB and Ti. Additionally, the composition optimization of the Ag-Cu-Ti alloy to braze CBN grains was carried out[13-16].

In this study, monolayer brazed CBN abrasive wheels are utilized to creep feed profiled grind cast nickel-based superalloy K424 for fabricating straight grooves, the outcome of which is projected to have large application in high-efficiency profiled machining of aeroengines blade roots in a near future. It is known from the theory of metal cutting that the investigation of surface integrity is the most effective way of understanding machining characteristics of a material. Measurement of machining characteristics of nickel-based superalloys represents one of the most important aspects in the analysis of machining processes. Therefore, the present article reports on the investigation of grindability (e.g. grinding force and temperature, specific grinding energy) and surface integrity (e.g. size stability, surface topography, microhardness, microstructure, and residual stress as well) of K424 superalloy in creep feed grinding with brazed CBN abrasive wheels.

2. Experimental Material and Procedure

2.1. Workpiece material and abrasive wheels

Cast nickel-based superalloy coded as K424 was used as the workpiece material in this study. This kind of nickel-based superalloys is the vital material for turbine blades, parts of aeroengine. The chemical composition and mechanical properties of K424 superalloy are given in Table 1 and Table 2, respectively[17]. Obviously, the content of Ti and Al in K424 superalloy is higher than that of other nickel-based superalloys such as GH4169 (Inconel 718). Moreover, K424 superalloy has high strength and good ductility. It is regarded as one of the most difficult-to-cut materials with the smallest relative cutting coefficient[18].

Table 1 Chemical composition of cast nickel-based superalloy K424

Element	Chemical Composition/wt%	
	Minimum	Maximum
C	0.14	0.20
Cr	8.50	10.50
Co	12	15
W	1.0	1.8
Mo	2.7	3.4
Al	5.0	5.7
Ti	4.2	4.7
Nb	0.5	1.0
V	0.5	1.0
Fe		2.0
Ni	Balance	

Table 2 Mechanical properties of cast nickel-based superalloy K424

Property	Value	
	20 °C	800 °C
Tensile strength /MPa	1010	935
Yield strength /MPa	755	770
Hardness /HRC	37.2	
Thermal conductivity /($W \cdot m^{-1} \cdot °C^{-1}$)	10.85	21.95
Density /($kg \cdot m^{-3}$)	8 200	
Linear thermal expansion /(10^{-6} °C^{-1})	14.1	

The brazed CBN abrasive wheels were manufactured at the brazing temperature of 920 °C for the dwell time of 5 min, as displayed in Fig.1. It had the segmented structure with a slot-ratio of 0.75. The wheel size was 265 mm in diameter and 4.5 mm in width of the working zone. AISI 1045 steel was utilized as the tool substrate. $(Ag_{72}Cu_{28})_{95}Ti_5$ (wt%) alloy was applied as the bonding material of CBN grains and tool substrate. The wheel was made of 80/100 US mesh CBN abrasive grains. Or equivalently, the average grain size was 150 μm. In particular, the CBN grains were distributed linearly in the working zones of the abrasive wheels (see Fig.1(b)).

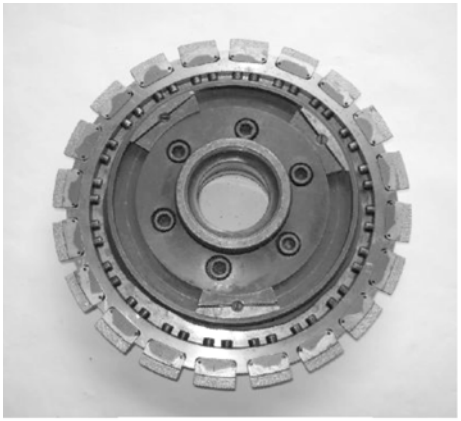

(a) Whole morphology

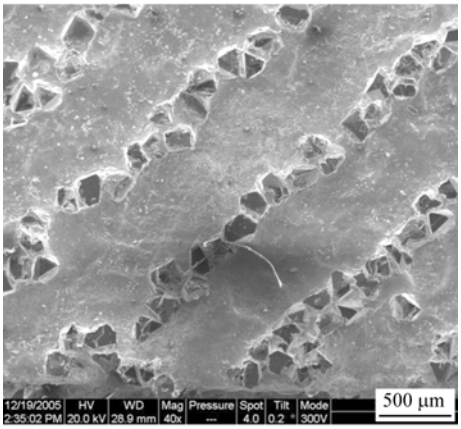

(b) Grain distribution

Fig.1 Morphology of brazed CBN abrasive wheel.

2.2. Experimental system

A MMD7125 precision surface grinding machine with a minimum workpiece speed of 0.1 m/min was em-

ployed. Experimental conditions are listed in Table 3. The experimental workpiece of K424 superalloy was a pair of small blocks with 60 mm in length, 10 mm in width, and 10 mm in height. Fig.2 shows the schematic illustration of the cross-section of the wheel-workpiece couple during creep feed profiled grinding. Thus, a straight groove may be fabricated. In the current experiments, the brazed CBN abrasive wheels were dressed with a single-point diamond dresser to ensure a sharp, clean tool surface. A set of initial grinding passes were carried out before the real grinding and date logging to stabilize the grinding performance.

Table 3 Conditions for grinding tests

Machine tool	MMD7125 precision surface grinding machine
Grinding mode	Plunge surface down-grinding
Abrasive wheels	Brazed CBN wheels
Average grain size/μm	150
Wheel speed v_s /(m·s^{-1})	17.5-25.0
Workpiece speed v_w / (m·min^{-1})	0.1-0.4
Depth of cut a_p/mm	0.08-0.20
Grinding width b/mm	4.5
Cooling mode	Emulsified liquid; 5% dilution; 90 L/min; Pressure at 0.4 MPa

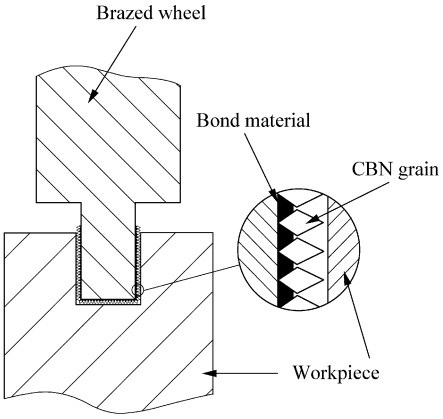

Fig.2 Schematic illustration of creep feed profiled grinding.

In order to explore fully the creep feed grinding process of K424 superalloy, the vertical and horizontal forces, F_V and F_H, were measured using a piezoelectric transducer-based type dynamometer (type Kistler 9265B), coupled to charge amplifiers and a PC running Dynowear software. For each set of process parameters, three grinding passes were undertaken to ensure the reliable machining results. At the same time, a constantan wire-workpiece semi-natural thermocouple was employed to measure grinding zone temperature. The grinding temperature signal was captured and recorded directly by HP3562 dynamic signal analyzer. Constantan wire was very thin with its diameter 0.02 mm and its response was rapid enough to record the temperatures caused by individual abrasive grains. Because the method to measure the grinding force and temperature in this work is similar to those applied in the corresponding literature[19-22], it is not described and illustrated in detail.

2.3. Testing method

Firstly, the cross-section profile of the ground samples was observed using KH-7700 optical microscope. The surface roughness of the samples was measured using a MAHR perthometer M2 surface roughness tester. The topography of the ground surface was detected with a QUANTA 200 scanning electron microscope (SEM) in a secondary electron (SE) mode. The residual stresses were evaluated using the ψ tilt X-ray method by means of a XD-3A diffractometer with Cu Kα radiation. The measured zone of the ground surface was 6 mm×20 mm.

Secondly, the ground samples were sectioned perpendicular to the grinding direction. Then the sectioned surfaces were polished. The hardness of the sub-surface was measured using a HXS-1000A micro-hardness tester at the load of 100 g for the dwell time of 15 s.

Finally, the polished samples were etched using the solution containing 6 vol% HF, 50 vol% HNO_3 and balance water. The metallurgical images of the sub-surface and the bulk material of the ground components were recorded with a KH-7700 optical microscope.

3. Grindability of Cast Nickel-based Superalloy K424

3.1. Grinding force

Generally, grinding force comprises four elements including cutting, ploughing, sliding and coolant dynamics[23]. The grinding force, to a vast extent, affects the machined surface roughness, the work hardening, the power consumption, the heat flux at the contact zone between the abrasive wheel and the workpiece, the gradient residual stresses, the surface defects as well as the wear of the abrasive grains[24-25]. On this basis, for K424 superalloy, it is necessary to express the relationships between the grinding forces and the process parameters, i.e. wheel speed, workpiece speed, and depth of cut.

In a creep feed grinding process, because the depth of cut is large, the grinding force components were always calculated by assuming that the average resultant grinding force acts at a middle point of the contact arc between the wheel and the workpiece. The normal grinding force F_n and the tangential grinding force F_t are described as[26]

$$F_n = F_V \cos\theta - F_H \sin\theta \quad (1)$$

$$F_t = F_V \sin\theta + F_H \cos\theta \quad (2)$$

where F_V is the measured vertical force, F_H the measured horizontal force, θ the included angle between the vertical force perpendicular to the

workpiece and the normal force vertor acting on the grinding zone, which may be written as

$$\theta = \sqrt{a_p / d_s} \tag{3}$$

where a_p is the depth of cut, and d_s the wheel diameter.

Fig.3 illustrates the representative grinding force curves measured under the condition of a wheel speed of 22.5 m/s, a workpiece speed of 0.1 m/min and a depth of cut of 0.2 mm. Where F is the grinding force, t is time. A series of grinding tests with different process parameters was undertaken in this investigation. Fig.4 demonstrates the measured grinding force as functions of wheel speed, workpiece speed and depth of cut, respectively. It is found that the increase in wheel speed leads to the slight decrease in both normal and tangential forces, as shown in Fig.4(a). However, a faster workpiece speed results in a larger grinding force, and the increase in depth of cut also induces a greater grinding force (see Fig.4(b) and Fig.4(c)). This is attributed to the fact that the the increase in workpiece speed and depth of cut resulted in the increase in the undeformed chip thickness[27]. At the same time, the magnitude of the normal force is significantly greater than that of the tangential force. For example, seen from Fig.4(c), when the depth of cut is increased from 0.08 mm to 0.20 mm, the normal force has been raised rapidly from 12 N to 28 N, while the tangential grinding froce is merely increased from 9 N to 13 N. Under such condition, the force ratio of F_n versus F_t is increased remarkably from 1.3 to 2.2.

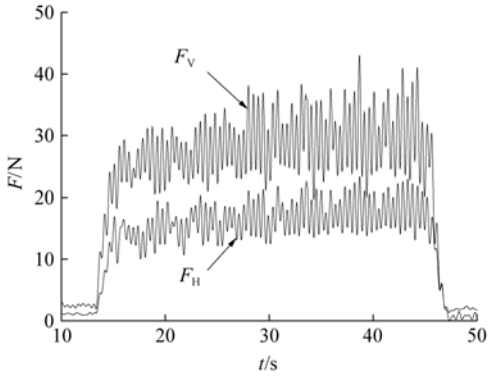

Fig.3 Typical grinding force signal of brazed CBN wheels.

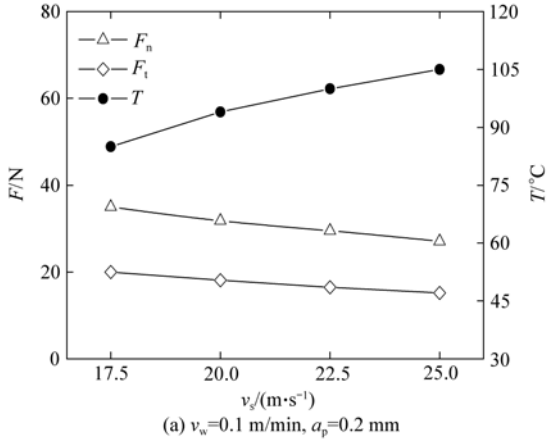

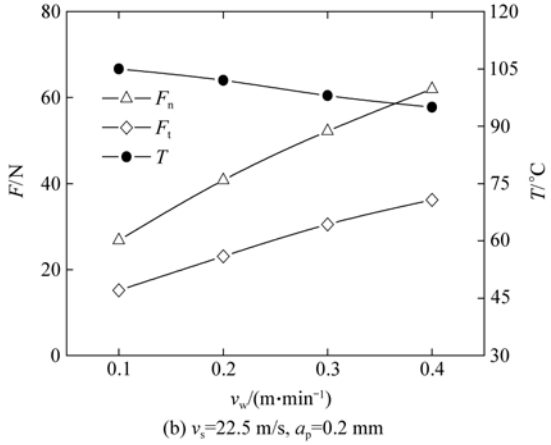

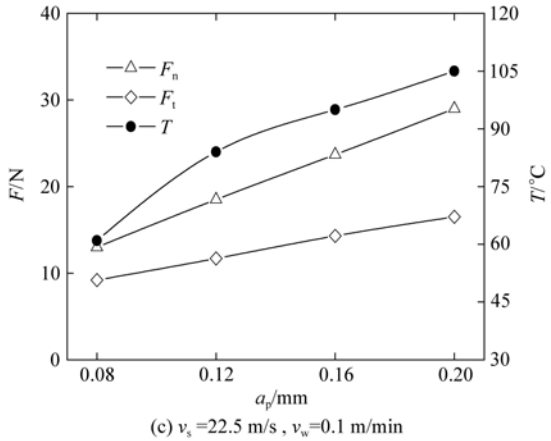

Fig.4 Influence of process parameters on grinding force and temperature.

3.2. Specific grinding energy

During grinding, specific energy is one of the most important grindability indices. It can be calculated with the use of the process parameters and the tangential grinding force measured in the experiment, as follows[28]:

$$u = \frac{F_t v_w}{v_s a_p b} \tag{4}$$

where b is the width of working zone of the grinding wheels, i.e., 4.5 mm in this investigation.

On the other hand, based on the geometrical characteristics of the chip formation, the maximum underformed chip thickness of the segmented grinding wheels is written as

$$a_{g,max} = \left(\frac{4 v_w}{\eta v_s N_d C} \sqrt{a_p / d} \right)^{1/2} \tag{5}$$

where N_d is the active cutting point density (6 mm^{-2} in this work), η the slot-ratio, i.e., 0.75 in this investigation, C a constant correlated with the angle of the grain tip. For the grain with the size of 150 μm, it is taken to be 6.928.

According to the grinding force and the process parameters shown in Fig.4, the experimental specific energy for creep feed grinding K424 superalloy is obtained

and plotted against the undeformed chip thickness, as displayed in Fig.5. With the application of the least squares curve-fitting technique to the experimental data, specific energy in this investigation is represented by

$$u = 128.99 a_{g,max}^{-1.027} \quad (6)$$

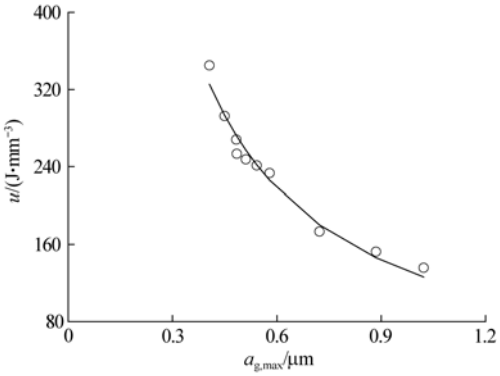

Fig.5 Relationship between specific grinding energy and underformed chip thickness.

Seen from Fig.5, the specific grinding energy of K424 superalloy is high up to 200-300 J/mm^3. Compared with other nickel-based superalloys also used for turbine blades, such as Udimet 520 and Inconel 713C, the specific grinding energy is only 130-160 J/mm^3 and 80-120 J/mm^3, respectively, in the case of the nearly identical undeformed chip thickness[29]. This implies that the grindability of K424 superalloy is much worse than that of Udimet 520 and Inconel 713C, though the latter are also called the most difficult-to-cut materials.

On the other hand, the specific grinding energy of cast nickel-based superalloy K424 has been gradually decreased with increase in $a_{g,max}$. This can be explained from the viewpoint of the abrasive-workpiece interaction. Just as reported in the previous work[30], the major phenomenon for chip formation during grinding is sliding, ploughing and cutting. In the case of small undeformed chip thickness, high specific grinding energy of K424 superalloy is mainly attributed to high ploughing and sliding energies. This is expended in grinding in excess of energy of chip formation by cutting. However, when the undeformed chip thickness is increased, the percentage contributions from sliding and ploughing diminish and thus specific grinding energy decreases with the undeformed chip thickness as well.

3.3. Grinding temperature

Grinding of nickel-based superalloys is a mechanical process that involves a great amount of energy per unit volume of removed material. This energy is almost all converted into heat, perhaps causing a significant rise of the temperature above 700 °C in a traditional plunge surface grinding process of DZ4 and GH4169 superalloy[19-20]. Therefore, the ground surface of the workpiece always experiences rapid thermal cycles, while the rest of the part remains at lower temperatures. The increased temperature can have harmful effects on the workpiece material, such as thermal deflection, burnout, surface cracking and residual stress[31].

A representative grinding temperature signal measured using the grindable thermocouple is displayed in Fig.6. The temperature response recorded by the foil/workpiece thermocouple is composed of two parts, a background temperature and periodic flash temperature impluses at the wheel rotational frequency. It has been suggested that flash temperature may be associated with the cutting action at individual grain cutting points[22]. In this study, the ginding temperature means the temperature increase on the workpiece surface, that is, the grinding zone temperature during creep feed grinding. The highest temperature at the given condition was approximately 105 °C.

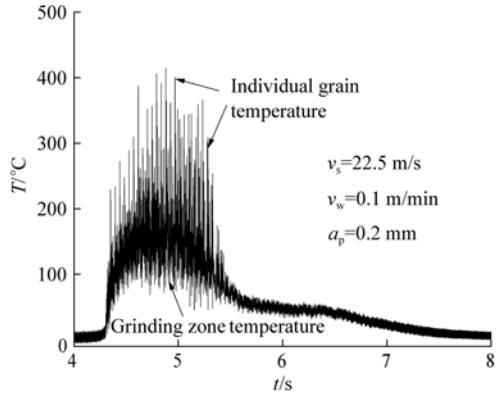

Fig.6 Typical temperature signal during creep feed grinding.

The values of grinding temperature for K424 superalloy are plotted against the process parameters in Fig.4. It is seen that the grinding temperature is increased with the increase in both the wheel speed and the depth of cut in the current investigation. However, the grinding temperature decreases with increase in the workpiece speed. This phenomenon is due to the change of the undeformed chip thickness of K424 superalloy during grinding.

According to Eq.(5), the increase in wheel speed leads to a reduction in the undeformed chip thickness. Thus, the chips become smaller. The corresponding material deformation energy is increased. Moreover, the quantity of the grains ploughing and sliding on the workpiece surface becomes larger. The friction behavior between the wheel and the workpiece gets severe. Therefore, the grinding temperature is increased. On the other hand, when the workpiece speed is heightened, the grinding heat is released conveniently though the maximum undeformed chip thickness is still increased. That is, high workpiece speed can substantially reduce the proportion of energy conducted into the workpiece.

It has to be noticed that, though the specific grinding energy of K424 superalloy is high up to 200-300 J/mm^3, the highest grinding temperature of K424 superalloy is merely about 100 °C in the current

investigation. This favorable phenomenon is not only determined by the fluid film burn-out effect of the coolant in creep feed grinding[32], but also contributes to the following factors, e.g. excellent cutting ability of CBN abrasive grains, efficient chip stroage space of the tools, good thermal conductivity property among the CBN grains, the bonding layer of Ag-Cu-Ti alloy and the tool substrate of AISI 1045 steel.

4. Surface Integrity of Ground Grooves of Cast Nickel-based Superalloy K424

4.1. Dimensional accuracy of ground grooves

Based on the experimental results of grinding force and temperature mentioned above, creep feed profiled grinding of K424 superalloy was finally carried out with a combination of the process parameters, i.e. $v_s = 22.5$ m/s, $v_w = 0.1$ m/min, $a_p = 0.2$ mm. Grinding tests were stopped at stock removal of 4 050 mm^3. Accordingly, three grooves with the length of 60 mm and depth of 5 mm were fabricated. At this time, the brazed CBN wheels still had good machining performance.

Fig.7 presents the typical morphology of the ground grooves. For evaluating the dimensional accuracy, the groove width was measured at the entrance and at the departure, respectively. The results are listed in Table 4. Obviously, the requirement of the expected dimensional accuracy has been fulfilled.

The comparison in the cross-sectional profile of the ground grooves is displayed in Table 5. It is found that

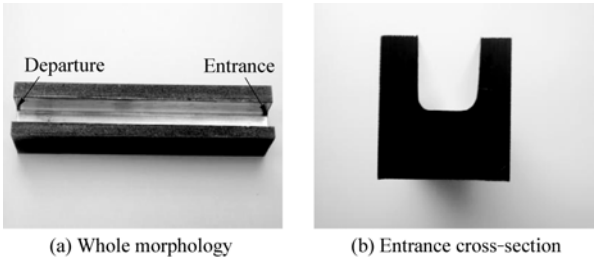

Fig.7 Typical morphology of ground grooves.

the corner profile formed in creep feed grinding with brazed CBN abrasive wheel remains nearly in the initial state up to the stock removal of 4 050 mm^3. More important, the corner radius in the bottom of the grooves is maintained constantly at 0.50 mm both at the entrance and at the departure. As reported in the previous literature, the profile wear and the radial wear of the applied abrasive wheels affect significantly the shape and accuracy of the ground grooves during creep feed profiled grinding[26]. The profile wear is the changes of shape of the profile formed on the grinding wheel as a consequence of the wheel wear. According to the experimental results in Table 5, it is known that the brazed CBN abrasive tools give less profile wear, and therefore better form retention. This is contributed to the fact that the very high hardness of CBN abrasive grains provides good size-holding ability for the CBN grinding. As a result, brazed CBN abrasive wheels are suitable for application with the requirement of high size stability in creep feed profiled grinding of K424 superalloy.

Table 4 Width variance in cross-sectional profile of ground grooves

Sample No.	Entrance width /mm	Departure width /mm	Designed width /mm	Entrance tolerance /mm	Departure tolerance /mm	Groove tolerance /mm
1	4.54	4.55				
2	4.53	4.53	$4.50^{+0.05}_{-0.05}$	$4.50^{+0.04}_{+0.02}$	$4.50^{+0.05}_{+0.03}$	$4.50^{+0.05}_{+0.02}$
3	4.52	4.54				

Table 5 Morphology variance in cross-sectional profile of ground grooves

Corner	Stock removal /mm^3		
	1 350	2 700	4 050
Corner at the entrance			
Corner at the departure	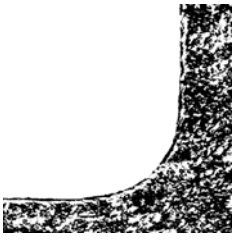	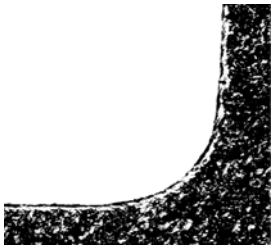	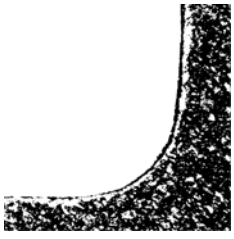

4.2. Surface topography

The quality of the surface generated by grinding determines many workpiece characteristics sush as the minimum tolerances, the lubrication effectiveness and the component life, among others[33]. When the workpiece is machined using the conventional milling and grinding method, it is not easy to meet the surface quality requirements.

Figs.8(a)-8(b) display the typical surface morphology of the workpiece ground under the condition of v_s=22.5 m/s, v_w=0.1 m/min, a_p=0.2 mm. Here, the surface roughness R_a is 1.0 μm, which is lower than the requirement provided in the corresponding literature (R_a below 2 μm)[9]. A lower surface roughness on a component tends to induce higher fatigue strength as compared to a coaser surface.

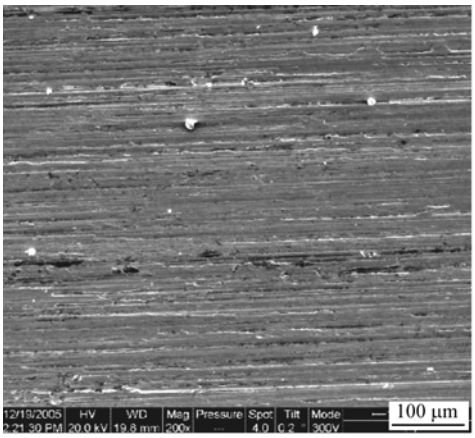

(a) Whole

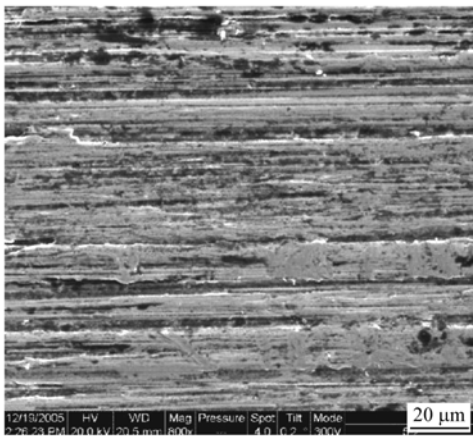

(b) Regional

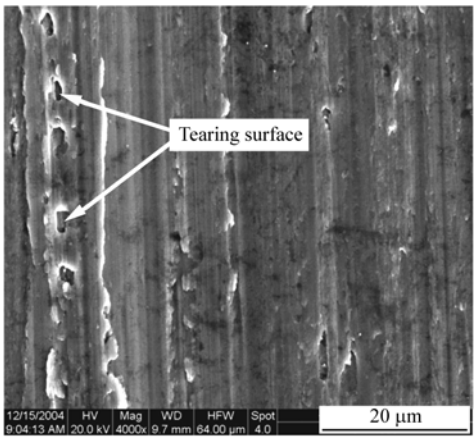

(c) Tearing surface

Fig.8 Typical topography of ground surface.

Additionally, a ground surface may be characterized by clean cutting paths and plowed materials to the sideway[33]. The feed mark, which is a natural defect because of infeeding, is observed at all the ground surface. Fig.8(b) shows the representive image of the feed marks. Particularly, the severity of grinding condition and the progressive wear of the CBN grains produce more significant feed mark on the machined surface. If the workpiece speed is increased further to 0.3 m/min, the tearing surface is randomly found on the ground surface, as demonstrated in Fig.8(c).

As is well known, in the creep feed grinding process, three bodies are contacted in sliding direction, i.e. abrasive grains, machined surface and a small part of the bonding layer of the brazed CBN wheels. Considering that the CBN grains are much harder than the workpiece material, they slide between the wheel and the machined surface. At last, the grains scratch and tear away the ground surface (Fig.8(c)). Consequently, it is thought that the combination of the beneficial effects of the brazed CBN wheels and the optimum grinding parameters makes the generation of defect-free machined surface.

4.3. Microhardness and microstructure alteration of sub-surface

In the course of grinding, once the workpiece material is subjected to high grinding temperature and large grinding pressure, a competing process between thermal softening and work hardening happens. For instance, when nickel-based superalloys and titanium alloys are machined with vitrified or electroplated superabrasive wheels, the rate of thermal softening behavior is always much greater than that of the work hardening effects in the process of the plastic deformation and the microstructure alteration of the sub-surface[6]. As a result, the soft sub-surface is formed, and the mechanical properties of the workpiece material perhaps deteriorate.

In order to analyze the sub-surface alteration of the ground grooves, the microhardness is measured using the Vickers method with $HV_{0.1}$ on the side surface and bottom surface of the grooves in Fig.7. Especially, the measurement of the hardness was conducted five times at every 5 μm up to 80 μm below the ground surface and the average hardness value for each depth was recorded. The results in terms of hardness versus the depth below the side surface and the bottom surface of the ground grooves are plotted in Fig.9. Apparently, no soft region but hard one exists on the sub-surface of the ground components. That is, workpiece burning has been avoided. The maximum hardness value, about 540 $HV_{0.1}$, is arrived at a depth of 10 μm. It is approximately 46% higher than the bulk material

hardness of 380 $HV_{0.1}$. After the peak point has been obtained, the hardness value decreases gradually until it attains the bulk material hardness at about 30 μm below the ground surface. Then, minor fluctuation has been observed up to a 80 μm below the surface. The same trends of the hardness distribution in the corner zone have been found in the current investigation.

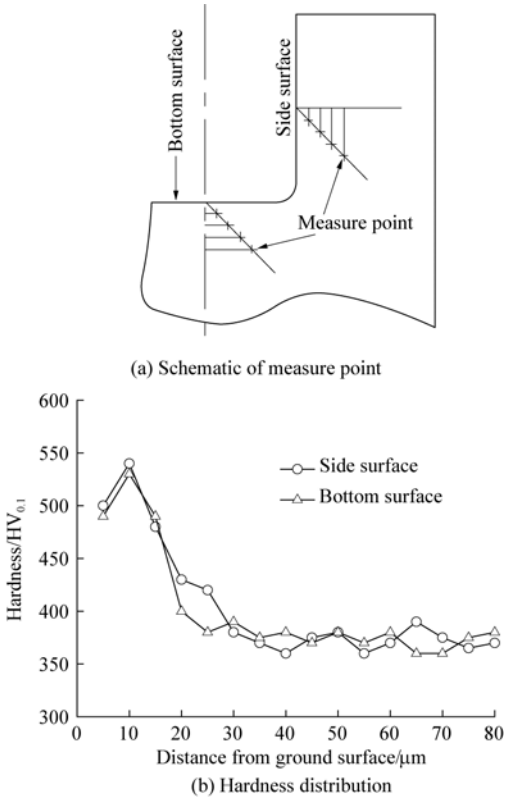

Fig.9 Hardness distribution on sub-surface of ground grooves.

The phenomenon mentioned above is attributed to that, during creep feed grinding, the highest hardness value of the sub-surface zone is always formed at the position, where the most drastic plastic deformation takes place due to the materials removal under high grinding pressure. Moreover, this special position is dependent on the maximum ratio of the normal grinding force F_n to the tangential grinding force F_t[34-35]. The larger the ratio of F_n/F_t is, the farther to the ground surface the position of the most drastice plastic deformation becomes.

The representative optical metallurgical image of the ground K424 superalloy is displayed in Fig.10. In particular, the metallurgy samples were carefully prepared to hinder smearing on the machined region. According to Fig.10(a), no microcrack is formed. Compared with the typical microstructure of the bulk material of K424 superalloy (Fig.10(b)), that is, γ phase, γ' and γ'' ones, the microstructure on the sub-surface region of the ground samples tends to exhibit plastic deformation and crystal lattice distortion to a small extent. This is the reason of the work hardening of the sub-surface. In fact, the drastic plastic deformation does occur from a single droplet which has been pressed through the gap between the cutting edge of the CBN grains and the ground material, and smeared over the ground surface[3]. Therefore, the plastic deformation and induced work hardening of the sub-surface may be controlled by means of adjusting the grinding condition and alleviating the wheel wear. In order to heighten the material removal rate and further improve the machining quality of the ground components, it is necessary to discuss the wheel wear mechanisms during creep feed grinding with brazed CBN abrasive wheels in the subsequent work.

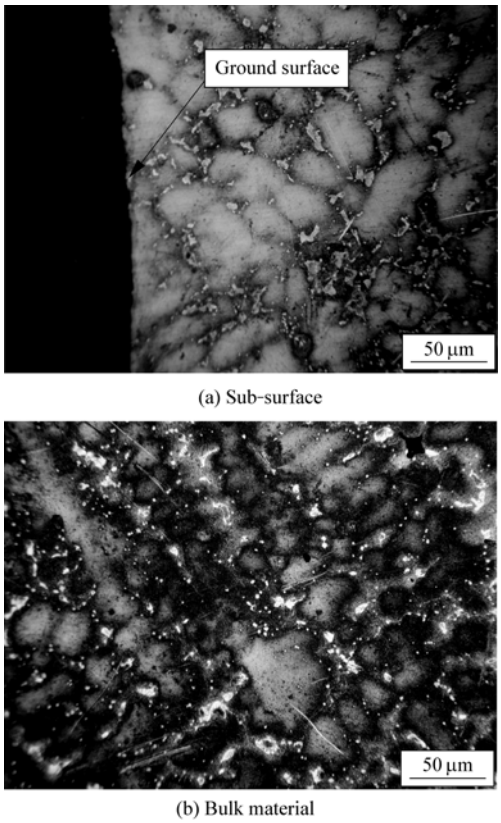

Fig.10 Microstructure alteration of sub-surface and bulk material.

4.4. Residual stresses on ground surface

Low residual stress after grinding is an important requirement for surface integrity of stress sensitive components, i.e. the turbine blade roots. When the grooves are machined using the traditional grinding and milling technique, it is possible to form a tensile residual stress up to 40 MPa in the sub-surface. The subsequent service life is therefore reduced under stress corrosion or fatigue conditions.

Among the three grinding parameters, the depth of cut has the most important influence on the residual stresses during creep feed grinding. For the reason, the stresses in the direction parallel to the grinding direction, σ_x, and that perpendicular to the grinding direction, σ_y, are measured against the depth of cut. The result is plotted in Fig.11.

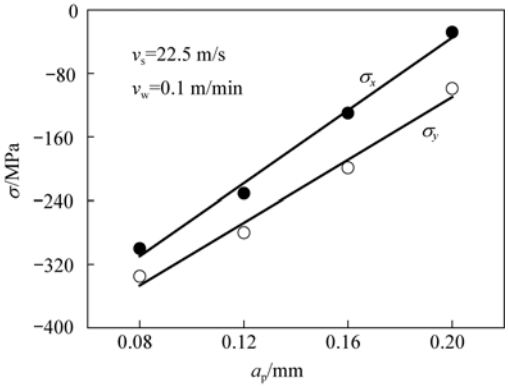

Fig.11 Residual stresses of ground surface against depth of cut.

Seen from Fig.11, the compressive residual stresses remain in both direction on the ground surface. The highest comressive stress value is obtained for a depth of cut of 0.08 mm. In this case, the residual stress measured in the grinding direction is σ_x= −300 MPa and that in the perpendicular direction is σ_y= −340 MPa. With the increase in depth of cut, the values of the compressive stresses are decreased. Moreover, the compresses stresses in the direction perpendicular to the grinding direction are always larger than those in the direction parallel to the grinding direction. When the depth of cut is 0.2 mm, the compressive stress value of σ_x and σ_y are −40 MPa and −120 MPa, respectively. This corresponds to a dominance of the mechanical effects comparatively to the thermal effects during the chip formation at the grinding zone[36].

It is known that the residual stresses in a ground surface are primarily generated due to the effects as follows: thermal expansion and contraction during grinding, phase transformations due to high grinding temperature, and plastic deformation caused by the cutting edges of the abrasive grains[37]. Because the grinding temperature of K424 superalloy with brazed CBN abrasive wheels is as low as about 100 °C in this work, the thermal effect may be neglected. Therefore, the effects generating residual stresses are governed by the wheel-workpiece mechanical interactions. In other words, the variance in the physical properties of the machined surface is attributed mainly to the plastic deformation resulted from the grinding pressure. In the area around the tip of the cutting edge of the CBN grain, the compressive level has to be very high since this is the only way to ensure that the ground material plastifies to a enough degree to allow chip formation. The mechanical stresses of high level being exerted on the surface of the workpiece tend to induce compressive residual stresses[38]. However, with the increase in depth of cut, the burnishing and scraping effects between the CBN abrasive grains and the K424 superalloy workpiece are weakened, the magnitude of the compressive residual stresses in the ground surface is therefore decreased gradually.

5. Conclusions

(1) During creep feed grinding cast nickel-based superalloy K424 with brazed CBN wheels, the grinding temperature may be effectively controlled at approximately 100 °C though the specific grinding energy is high up to 200-300 J/mm^3.

(2) Straight grooves of K424 superalloy are fabricated successfully using the creep feed profiled grinding technique with a combination of the machining parameters of v_s=22.5 m/s, v_w=0.1 m/min and a_p=0.2 mm.

(3) Creep feed grinding with brazed CBN abrasive wheels result in good surface integrity without any burn and cracks. Reducing the thermal input in the ground surfaces reduces metallurgical damage and forms favorable compressive residual stresses. No thermal softening but work hardening effect takes place in the sub-surface of the ground components.

References

[1] Soo S L, Ng E G, Dewes R C, et al. Point grinding of nickel-based superalloys. Industrial Diamond Review 2002; 62(2): 109-116.

[2] Xu X P, Yu Y Q, Xu H J. Effect of grinding temperatures on the surface integrity of a nickel-based superalloy. Journal of Materials Processing Technology 2002; 129(1-3): 359-363.

[3] Osterle W, Li X P. Mechanical and thermal response of a nickel-base superalloy upon grinding with high removal rates. Materials Science and Engineering A 1997; 238(2): 357-366.

[4] Zhang L C, Suto T, Noguchi H, et al. A study of creep-feed grinding of metallic and ceramic materials. Journal of Materials Processing Technology 1995; 48(1-4): 267-274.

[5] Liao T W, Li K, Mcspadden S B, et al. Wear of diamond wheels in creep-feed grinding of ceramic materials I. mechanisms. Wear 1997; 211(1): 94-103.

[6] Hood R, Lechner F, Aspinwall D K, et al. Creep feed grinding of gamma titanium aluminide and burn resistant titanium alloys using SiC abrasive. International Journal of Machine Tools & Manufacture 2007; 47(9): 1486-1492.

[7] Abdullah A, Pak A, Farahi M, et al. Profile wear of resin-bonded nickel-coated diamond wheel and roughness in creep-feed grinding of cemented tungsten carbide. Journal of Materials Processing Technology 2007; 183(2-3): 165-168.

[8] Maksoud T M A. Heat transfer model for creep-feed grinding. Journal of Materials Processing Technology 2005; 168(3): 448-463.

[9] Aspinwall D K, Soo S L, Curtis D T, et al. Profiled superabrasive grinding wheels for the machining of a nickel based superalloy. Annals of the CIRP 2007; 56(1): 335-338.

[10] Teicher U, Kunanz K, Ghosh A. Performance of diamond and CBN single-layered grinding wheels in grinding titanium. Materials and Manufacturing Processes 2008; 23(3): 224-227.

[11] Ghosh A, Chattopadhyay A K. On cumulative depth of touch-dressing of single layer brazed CBN wheels with regular grit distribution pattern. Machining Science and

Technology 2007; 11(2): 259-270.
[12] Chattopadhyay A K, Hintermann H E. On performance of brazed single-layer CBN wheel. Annals of the CIRP 1994; 43(1): 313-317.
[13] Yang C Y, Xu J H, Ding W F, et al. Grinding titanium alloy with brazed monolayer CBN wheels. Key Engineering Materials 2008; 359-360: 33-37.
[14] Ding W F, Xu J H, Shen M, et al. Joining of CBN abrasive grains to medium carbon steel with Ag-Cu/Ti powder mixture as active brazing alloy. Materials Science and Engineering A 2006; 430(1-2): 301-306.
[15] Elsener H R, Klotz U E, Khalid F A. The role of binder content on microstructure and properties of a Cu-base active brazing filler metal for diamond and CBN. Advanced Engineering Materials 2005; 7(5): 375-380.
[16] Ding W F, Xu J H, Fu Y C, et al. Delamination behavior and formation mechanism of the interfacial microstructure in the brazed joint of silver-copper-titanium alloy and cubic boron nitride grain. Chinese Journal of Mechanical Engineering 2008; 44(6): 61-65. [in Chinese]
[17] Editorial Committee. China aeronautical materials handbook. Beijing: Standards Press of China, 2002. [in Chinese]
[18] Xing L H, Chen X, Zhang D Y. Experimental study on the drilling of cast nickel-based super alloy K24. Proceedings of the 7th International Conference on Progress of Machining Technology. 2004; 90-95.
[19] Chen M, Li X T, Sun F H, et al. Studies on the grinding characteristics of directionally solidified nickel-based superalloy. Journal of Materials Processing Technology 2001; 116(2-3): 165-169.
[20] Ren J X, Yang M K, Li Y Q, et al. Grinding characteristics of nickel-based superalloy. Acta Aeronautica et Astronautica Sinica 1997; 18(6): 755-758. [in Chinese]
[21] Batako A D, Rowe W B, Morgan M N. Temperature measurement in high efficiency deep grinding. International Journal of Machine Tools & Manufacture 2005; 45(11): 1231-1245.
[22] Xu X P, Malkin S. Comparison of methods to measure grinding temperatures. Journal of Manufacturing Science and Engineering—Transactions of the ASME 2001; 123(2): 191-195.
[23] Liu Q, Chen X, Gindy N. Assessment of Al_2O_3 and superabrasive wheels in nickel-based alloy grinding. International Journal of Advanced Manufacturing Technology 2007; 33(9-10): 940-951.
[24] Amamou R, Ben F N, Fnaiech F. Improved method for grinding force prediction based on neural network. International Journal of Advanced Manufacturing Technology 2008; 39(7-8): 656-668.
[25] Liu Q, Chen X, Wang Y, et al. Empirical modelling of grinding force based on multivariate analysis. Journal of Materials Processing Technology 2008; 203(1-3): 420-430.
[26] Sunarto, Ichida Y. Creep feed profile grinding of Ni-based superalloys with ultrafine-polycrystalline CBN abrasive grits. Precision Engineering 2001; 25(4): 274-283.
[27] Xie G Z, Huang H. An experimental investigation of temperature in high speed deep grinding of partially stabilized zirconia. International Journal of Machine Tools & Manufacture 2008; 48(14): 1562-1568.
[28] Ren Y H, Zhang B, Zhou Z X. Specific energy in grinding of tungsten carbides of various sizes. Annals of the CIRP 2009; 58(1): 299-302.
[29] Suto T, Waida T, Noguchi H, et al. Wheel designs for grinding. Industrial Diamond Review 1990; 50(538): 133-136.
[30] Ghosh S, Chattopadhyay A B, Paul S. Modelling of specific energy requirement during high-efficiency deep grinding. International Journal of Machine Tools and Manufacture 2008; 48(11): 1242-1253.
[31] Kim H J, Kim N K, Kwak J S. Heat flux distribution model by sequential algorithm of inverse heat transfer for determining workpiece temperature in creep feed grinding. International Journal of Machine Tools & Manufacture 2006; 46(15): 2086-2093.
[32] Jin T, Rowe W B, McCormack D. Temperatures in deep grinding of finite workpieces. International Journal of Machine Tools & Manufacture 2002; 42(1): 53-59.
[33] Hecker R L, Liang S Y. Predictive modeling of surface roughness in grinding. International Journal of Machine Tools & Manufacture 2003; 43(8): 755-761.
[34] Furukawa Y, Ohishi S, Shiozaki S. Selection of creep feed grinding condition in view of workpiece buring. Annals of the CIRP 1979; 28(1): 213-218.
[35] Ma S Y, Xu J H, He X C, et al. On the characterization of hardening of grinding affected layer of steels in hard state. Acta Metallurgica Sinica 2003; 39(2): 168-171. [in Chinese]
[36] Ben F B, Ben F N, Sidhom H, et al. Effects of abrasive type cooling mode and peripheral grinding wheel speed on the AISI D2 steel ground surface integrity. International Journal of Machine Tools & Manufacture 2009; 49(3-4): 261-272.
[37] Chen X, Rowe W B, McCormack D. Analysis of the transitional temperature for tensile residual stress in grinding. Journal of Materials Processing Technology 2000; 107(1-3): 216-221.
[38] Rech J, Moisan A. Surface integrity in finish hard turning of case-hardened steels. International Journal of Machine Tools & Manufacture 2003; 43(5): 543-550.

Biography:

Ding Wenfeng Born in 1978, associate professor, he received Ph.D. degree from Nanjing University of Aeronautics and Astronautics in 2006. Now he works as a teacher there. His main research interest lies in fabrication and application of brazed CBN abrasive wheels for high-performance grinding of difficult-to-cut materials.
E-mail: dingwf2000@vip.163.com